UNIVERSITY OF AMSTERDAM

UvA-DARE (Digital Academic Repository)

Setting the scale

The balance between complement factor H and its related proteins in health and disease

Pouw, R.B.

Publication date
2018
Document Version
Other version
License
Other

Link to publication

Citation for published version (APA):
Pouw, R. B. (2018). *Setting the scale: The balance between complement factor H and its related proteins in health and disease*. [Thesis, externally prepared, Universiteit van Amsterdam].

General rights
It is not permitted to download or to forward/distribute the text or part of it without the consent of the author(s) and/or copyright holder(s), other than for strictly personal, individual use, unless the work is under an open content license (like Creative Commons).

Disclaimer/Complaints regulations
If you believe that digital publication of certain material infringes any of your rights or (privacy) interests, please let the Library know, stating your reasons. In case of a legitimate complaint, the Library will make the material inaccessible and/or remove it from the website. Please Ask the Library: https://uba.uva.nl/en/contact, or a letter to: Library of the University of Amsterdam, Secretariat, P.O. Box 19185, 1000 GD Amsterdam, The Netherlands. You will be contacted as soon as possible.

UvA-DARE is a service provided by the library of the University of Amsterdam (https://dare.uva.nl)

Download date:18 Nov 2026

3

Antibody-mediated potentiation of complement regulator factor H protects human endothelial cells from complement attack in aHUS sera

Richard B. Pouw, Mieke C. Brouwer, Marlon de Gast, Anna E. van Beek, Lambertus van den Heuvel, Christoph Q. Schmidt, Arie van der Ende, Pilar Sánchez-Corral, Taco W. Kuijpers, and Diana Wouters

Submitted

Abstract

Mutations in the gene encoding for complement regulator factor H (FH) severely disrupt its normal function to protect human cells from unwanted complement activation, resulting in diseases such as atypical hemolytic uremic syndrome (aHUS). Treatment by inhibiting the terminal complement pathway has proven to be successful, but at the same time fails to preserve the protective role of complement against pathogens. To improve complement regulation on human cells without interfering with the antimicrobial activity, we identified an anti-FH monoclonal antibody (mAb) that induced increased FH-mediated complement regulation on human endothelial cells, while it preserved the complement-mediated killing of bacteria. Moreover, this FH-activating mAb restored complement regulation in sera from aHUS patients carrying various heterozygous mutations in FH, known to impair FH function and dysregulate complement activation. Our results show that FH can become more active, allowing enhanced complement regulation on human cells, and provides a new possible strategy for therapeutic intervention in various complement-mediated diseases.

Introduction

Impaired regulation of complement on human surfaces can lead to severe inflammatory disease like atypical hemolytic uremic syndrome (aHUS). In aHUS, the imbalance in complement regulation and activation leads to complement deposition on human cells, particularly in the kidneys, causing severe vascular injury and end-stage renal failure[1–6]. The function of the pivotal complement regulator factor H (FH) is impaired in 20-30% of the aHUS patients, due to mutations or auto-antibodies[7]. FH is a 155 kDa glycoprotein consisting of twenty complement control protein (CCP) domains. FH inhibits complement activation by binding to C3b, both in fluid phase and deposited on human cells and tissues, blocking further complement activation through competition with complement factor B (FB) for C3b binding[8–10]. In addition, FH is a cofactor for complement factor I (FI), which degrades C3b into inactive C3b (iC3b). In principle, FH strictly protects human cells. It distinguishes human from foreign surfaces by recognizing, next to C3b, polyanionic residues specific for human cells[11–15].

While aHUS-associated FH mutations are found along the entire protein, the C-terminal CCP20 domain seems to be a hotspot for mutations and the target of most auto-antibodies[2,16], affecting the binding of FH to C3b and polyanionic residues[3]. Although the precise structure of FH remains elusive, it circulates as a monomeric protein folded back onto itself and seems to appear in different conformations[17–19]. Conformational changes in FH are suggested to play a role in its function, with the central domains of FH forming a loop that brings together the relatively distant binding sites in its N- and C-terminal domains[20,21]. The presence of a latent, less active conformation of FH has been suggested as an additional mechanism to avoid protecting foreign surfaces which do not activate FH, while human cells fully activate FH[22].

Since FH plays a crucial role in the regulation of complement on human cells, we investigated the possibility of enhancing FH activity to improve complement regulation on human cells. We have generated anti-human FH monoclonal antibodies (mAbs) and tested their effect on the complement regulatory activity of FH. Although most mAbs were inhibiting FH function, one mAb enhanced FH activity, resulting in more efficient complement regulation on human cells. Our results show FH function can be enhanced, supporting the hypothesis that FH circulates normally in a less active conformation.

Materials and Methods

Patients and controls

All sera were obtained with informed consent according to the local ethics committees in

accordance with the Declaration of Helsinki. Sera were from two Dutch aHUS patients (aHUS#1, aHUS#2) and nine patients from the Spanish aHUS registry (aHUS#3-aHUS#11) carrying different *CFH* variants. Functional data for Arg53Ser[23] (aHUS#7), Ser411Thr[24] (aHUS#10, also carrying a *CFHR1::CFH* hybrid gene), Val1007Leu[25] (aHUS#5), Trp1157Arg[26] (aHUS#6), Arg1182Lys[23] (aHUS#8), Trp1183Leu[27] (aHUS#3), Ser1191Leu[28] (aHUS#1), and Val1197Ala[3] (aHUS#9) mutations were described previously. The functional consequences of Val383Ala (aHUS#11), Glu847Val[7] (aHUS#4), and Tyr1058His (aHUS#2) are unknown.

A normal human serum (NHS) pool was obtained by pooling sera from 30 healthy donors, aliquoted and stored at -80°C until further use. Heat-inactivated NHS (HI-NHS) was obtained by incubating the NHS pool for 1 hour at 56°C while shaking. A NHS pool deficient of FHR-1 (*CFHR1*$^{-/-}$ pool) was obtained by pooling sera from 4 healthy donors carrying zero gene copies of *CFHR3* and *CFHR1* (previously determined by MLPA[29]). FH and C5 levels for each pool were determined by in-house assays (Sanquin Research and Sanquin Diagnostics). FH-depleted serum was generated by affinity-purification of FH from a healthy donor serum using anti-FH.16-coupled sepharose and collecting the flow through.

Proteins and reagents

Plasma-derived human FH, plasma-derived FI, purified C3b, purified iC3b and purified C3d were all purchased from CompTech (Tyler, TX, USA). In-house generated mouse mAbs directed against IL-6 and coagulation factor XII were used as IgG1 and IgG2a isotype controls, respectively. Eculizumab (Alexion Pharmaceutical, Cheshire, CT, USA) was obtained by collecting surplus from used Soliris® injection bottles. Sheep erythrocytes (E_S) were obtained from Håtunalab (Håtunaholm, Sweden). Rabbit erythrocytes (E_R) were obtained from Envigo (Huntingdon, UK). High performance ELISA buffer (HPE), poly-HRP-conjugated streptavidin and rat anti-mouse Kappa mAb (RM-19) were purchased from Sanquin Reagents (Amsterdam, the Netherlands).

Immunization and antibody characterization

Mouse immunization and generation of mAbs was performed as described previously[29], using plasma-derived human FH as immunogen. Isotypes were determined by an in-house IgG1 ELISA or with the use of the IsoStrip Mouse Monoclonal Antibody Isotyping Kit (Roche, Basel, Switzerland). Cross-reactivity towards FH-related (FHR) proteins was determined with recombinant FHR proteins obtained as previously described[29].

Epitope mapping and cross-reactivity of anti-FH.07

The location of the epitope of anti-FH.07 was determined using recombinant human FH fragments composed of multiple CCP domains (1-4, 1-7, 4-6, 6-8, 8-15, 12-13, 15-18, 15-19, 18-20 or 19-20). In short, 5 µg of anti-FH.07 was captured with 1 mg RM-19 coupled-

sepharose and incubated with 100 µL ($4*10^4$ counts/minute) of ^{125}I-labeled FH or fragments, O/N. The assay was performed in PBS with 0.1% (w/v) Tween-20 and 0.1% (w/v) BSA. Unbound fragments were washed five times with PBS with 0.1% (w/v) Tween-20. Sepharose-bound radioactivity was measured by counting for 30 seconds and corrected for total input (set to 100%).

In addition, an ELISA-based competition assay was used to confirm the epitope mapping. In short, anti-FH.07 was captured on a RM-19 coated microtiterplate to assure optimal binding conformation. Next, biotinylated FH, mixed with a 100-fold higher concentration of the indicated unlabeled recombinant FH-fragments, was incubated on the plate for 1 hour. Binding of biotinylated FH was determined by strep-poly HRP and the ELISA was developed as previously described. Using the same ELISA set-up, binding of 1 µg/mL biotinylated FH or recombinant human FHR proteins to anti-FH.07 was measured to determine possible cross-reactivity of anti-FH.07.

Generation of Fab' fragments

Intact mAbs, 1 mg/mL in 0.1 M citric acid-trisodium citrate buffer, pH 3.7, were incubated with pepsin (20 µg/mL, P-6887, Sigma-Aldrich, St. Louis, MO, USA) for 16 hours at 37°C. Next, 3 M NaCl and 1 M Tris were added and the pH was adjusted to 8.9. A protein A sepharose column was used to remove remaining intact antibodies and/or Fc fragments. Next, the fragments were reduced by incubation with 10 mM dithioerythritol for 1 hour. Subsequently free thiol groups were blocked with 20 mM iodoacetamide. Obtained Fab' fragments were dialyzed to PBS and cleavage efficiency was checked on SDS-PAGE. The concentration of obtained Fab' fragments was determined by measuring the $OD280_{nm}$ using a standard extinction coefficient of 14 (1% w/v solution).

C3 deposition on zymosan and LPS

Polysorp 96-wells microtiter plates (Nunc) were coated with either *Saccharomyces cerevisiae*-derived zymosan A (100 µg/mL, Z4250 Sigma-Aldrich) or *Salmonella typhosa* LPS (40 µg/mL, L-6386 Sigma-Aldrich) in PBS, O/N at RT. After washing with PBS + 0.1% (w/v) Tween-20, 10% (v/v) NHS was incubated in Veronal buffer (VB; 3 mM barbital, 1.8 mM sodium barbital, 145 mM NaCl, pH 7.4) containing 0.05% (w/v) gelatin, 5 mM $MgCl_2$, 10 mM EGTA and 0.1% (w/v) Tween-20 in the presence or absence of anti-FH mAbs or isotype controls at indicated concentrations. C3b deposition was detected with biotinylated mAb anti-C3.19 (0.55 µg/mL in HPE) followed by incubation with 0.01% (v/v) streptavidin conjugated with poly-HRP, in HPE for 1 hour. The ELISA was further developed using 100 µg/mL 3,5,3',5'-tetramethylbenzidine (TMB) in 0.1 M sodium acetate containing 0.003% (v/v) H_2O_2, pH 5.5. Substrate conversion was stopped by addition of 100 µL H_2SO_4 and absorbance was measured at 450 nm and corrected for the absorbance at 540 nm with a Synergy 2 Multi-Mode plate reader (BioTek

Instruments, Winooski, VT, USA). All ELISA steps were performed with a final volume of 100 µL per well.

Cofactor activity assay

Fluid phase FH cofactor activity was determined as described previously[30], with some adjustments. C3b (3 µg) was mixed with 200 ng FH and 90 ng FI in a total reaction volume of 20 µL and incubated at 37°C for 30 minutes. The reaction was stopped by adding 30 µL stop buffer (12.5 µL H_2O, 12.5 µL 4x NuPAGE LDS Sample Buffer and 5 µL 10x NuPAGE Reducing Agent, both from Invitrogen, Life Technologies, Carlsbad, USA) and heating the samples at 70°C for 10 minutes. To assess FH cofactor activity in the presence of anti-FH mAbs, FH was incubated with a four-fold excess of anti-FH mAbs (800 ng) in a total volume of 12.5 µL for 15 minutes at RT prior to the addition of FI and C3b. Degradation products of C3b were separated by SDS-PAGE under reducing conditions and visualized with PageBlue Protein Staining Solution (ThermoFisher Scientific, Waltham, MA, USA).

C3b/c ELISA

NHS (10%, v/v) was incubated with 50 µg/mL of the indicated mAbs at room temperature for 45 minutes. Complement activation was stopped by addition of ice-cold buffer containing 10 mM EDTA. C3 activation was measured using the C3b/c ELISA as described previously[31].

SPR

The surface plasmon resonance (SPR) experiments were performed using a BiaCore T200 (GE Healthcare) and research-grade CM5 sensor chips (GE Healthcare). For the assessment of the affinity of anti-FH.07, RM-19 was immobilized using standard amine-coupling. Two surfaces of the flow cells were activated for 7 minutes with a 1-to-1 mixture of 0.1 M N-hydroxysuccinimide and 0.1 M 3-(N,N-dimethylamino) propyl-N-ethylcarbodiimide at a flow rate of 5 µL/minute. RM-19, at a concentration of 20 µg/mL in 10 mM sodium acetate, pH 5.0, was immobilized at a target density of 4,000 RU on all flow cells. The surfaces were blocked with a 7 minutes injection of 1 M ethanolamine, pH 8.0. SPR experiments were performed at 25°C using a flow rate of 15 µL/minute and in PBS, pH 7.4, with 0.1% (w/v) Tween-20 (PBS-T) unless stated otherwise.

To assess binding affinity, 30 µg/mL anti-FH.07 was captured on one flow cell of the RM-19 coated chip during 60 seconds, corresponding with 80 RU, leaving the other flow cell blank as reference surface. After a stabilization period of 60 seconds, duplicate injections, in random order, of FH (155 kDa, >97% pure based on SDS–PAGE) or $FH_{18\text{-}20}$ (21.4 kDa, >99% pure based on SDS–PAGE) were injected over both flow cells with a 2-fold dilution concentration range starting at 200 and 150 nM, respectively. The complex was allowed to associate and dissociate for 600 seconds. After each FH injection, the surfaces were regenerated with a 5

second injection of 100 mM HPO_3 at 30 µL/minute and the process was repeated starting with the capturing of anti-FH.07.

To assess the binding of FH to C3b, iC3b or C3d in the presence of anti-FH.07, purified C3b (2,045 RU), iC3b (2,039 RU) or C3d (2,055 RU) were immobilized onto one of three flow cells using standard amine-coupling as described above. The remaining flow cell was used as reference surface for background subtraction and prepared by performing a coupling reaction without the addition of any protein. Duplicate injections, in random order, of FH at a two-fold dilution concentration range starting at 2 µM, were injected at 10 µL/minute over all flow cells and allowed to associate and dissociate for 60 seconds. The surfaces were regenerated with a 10 second injection of 1 M NaCl at 10 µL/minute. To assess the effect of anti-FH.07 on the binding affinity of FH, FH was diluted in PBS-T containing a surplus of anti-FH.07 Fab' fragments (4 µM). Data were collected at a rate of 10 Hz and corrected for the MW of FH (155 kDa) and the FH:anti-FH.07 Fab' fragment complex (205 kDa), respectively. All SPR data were analyzed using Scrubber (v2.0c, BioLogic)

Sheep erythrocyte hemolytic assay

FH functionality was determined with a hemolytic assay as described previously[27], with some adjustments. Pre-diluted human serum, either from healthy donors of aHUS patients, was mixed in a 1-to-1 ratio with E_S to reach the indicated final concentrations of serum and $1.05*10^8$ cells/mL in VB with 5 mM $MgCl_2$ and 10 mM EGTA, or VB with 10 mM EDTA as blank, followed by incubation at 37°C for 75 minutes while shaking. Lysis was stopped by adding 100 µL ice-cold VB with 20 mM EDTA followed by centrifugation (2.5 minutes, 1,800 RPM/471 RCF, 7°C). Hemolysis was measured as absorbance of the supernatants at 412 nm, corrected for background absorbance measured at 690 nm, and expressed as percentage of the 100% lysis control (E_S incubated with 0.6% (w/v) Saponin). In follow-up experiments, 20% (v/v) human serum was incubated with the indicated mAbs, prior to mixing it in a 1-to-1 ratio with E_s.

Rabbit erythrocyte hemolytic assay

E_R, corresponding to an absorbance at 412 nm of 2.00 (corrected for background absorbance at 690 nm) when 100% lysis occurs, were incubated with 10% (v/v) NHS and anti-FH.07 or eculizumab at indicated concentrations in VB supplemented with 5 mM $MgCl_2$ and 10 mM EGTA, in a final volume of 100 µL, at 37°C for 1 hour. After incubation, 100 µL of VB was added, followed by centrifugation (1.5 min, 2,500 RPM/654 RCF, 4°C). Hemolysis was measured as absorbance of 150 µL of the supernatants at 412 nm, corrected for background absorbance measured at 690 nm, and expressed as percentage of the 100% lysis control (E_R incubated with 0.6% (w/v) Saponin, corresponding with an A412/690 of 2.00).

Fluorescent imaging of C3b deposition on HUVECs

Confluent human umbilical vein endothelial cells (HUVECs; Lonza, Walkersville, MD, USA) were seeded onto 0.1% (w/v) gelatin-coated 12 mm coverslips (ThermoFisher Scientific) in EMB-plus medium supplemented with EGM-plus SingleQuots (Lonza) at 37°C, 5% CO_2, overnight. At the start of the experiment, the medium was refreshed and cells were allowed to rest for 1 hour at 37°C, 5% CO_2. Next, NHS, FH impaired NHS (containing anti-FH.09) or aHUS patient sera, pre-incubated with anti-FH.07 or isotype control for 15 minutes, were added to the cells (final concentrations: 10% (v/v) serum, 10 µg/mL anti-FH.09, and 75 µg/mL anti-FH.07 or isotype ctrl) and incubated for 1 hour at 37°C, 5% CO_2. Cells were fixed with 3% (w/v) paraformaldehyde (Merck Millipore, Billerica, MA, USA) in PBS containing 1 mM $CaCl_2$ and 0.5 mM $MgCl_2$, for 10 minutes after which the cells were washed and blocked with PBS + 2% (w/v) BSA for 15 minutes. Cells were stained in PBS + 0.5% (w/v) BSA with 1.25 µg/mL biotinylated WGA (Vector Laboratories, Burlingame, CA, USA) for 45 minutes, washed with PBS + 0.5% (w/v) BSA and stained with 0.004% (v/v) Hoechst (ThermoFisher Scientific), 5.8 ng/mL FITC-labelled anti-C3.19[32,33] and 1% (v/v) APC-conjugated streptavidin (BD Biosciences, San Jose, CA, USA) in PBS + 0.5% (w/v) BSA for 30 minutes. Cells were washed in PBS and mounted with 10% (v/v) Mowiol® 4-88 (Merck Millipore) + 2.5% (v/v) Dabco 33LV (Sigma Aldrich) + 25% (w/v) Glycerol, pH 8.5, onto microscope slides. Cells were imaged with a confocal microscope (40x oil emersion lens, LSM510 META, Carl Zeiss MicroImaging, Jena, Germany). For quantification of C3b deposition, cells were imaged with a widefield microscope (Axio Upright Examiner.Z1, Carl Zeiss MicroImaging) imaging an area of 10x10 frames (40x water lens), in a stack of 15-25 layers, per coverslip. Obtained frames were analyzed to obtain a maximum intensity projection per coverslip, subsequently used to determine mean fluorescence intensity of C3b deposition using ZEN, version 2.3 (Carl Zeiss).

Serum bactericidal activity assay

Bactericidal activity of NHS in the presence of anti-FH.07 or eculizumab was in principle determined as described previously[34,35]. One Shot® TOP10F' *Escherichia coli* (ThermoFisher Scientific) carrying the pcDNA3.1 vector (Invitrogen, conferring ampicillin/carbenicillin resistance) were grown in LB-medium containing 50 µg/mL carbenicillin to mid-logarithmic phase. The mid-log culture was diluted to OD_{600} = 0.001 in LB-medium and incubated with 75% (v/v) NHS or HI-NHS, with a final volume of 100 µL. Prior to incubation, eculizumab or anti-FH.07 were added to NHS as indicated, with final concentrations starting at 2 µM. Cultures were incubated at 37°C for 1 hour while shaking. Survival was determined by counting colony forming units (CFU) of 25 µL of undiluted up to 10^4-fold diluted (in LB) culture, plated on LB + 50 µg/mL carbenicillin agar plates and incubated at 37°C, O/N. The lower detection limit was 40 CFU/mL.

Survival of two clinical isolates of *Neisseria meningitidis*, 2996 (serogoup B) and 870486

(serogroup W), in NHS, in the presence of eculizumab or anti-FH.07, was determined using the same protocol, but using OD_{530} instead of OD_{600}, TSB-medium and Chocolate agar plates without selection antibiotic instead of LB-medium and LB-agar plates, diluting the cultures up to 10^6-fold for CFU counting, and growing the cultures at 37°C with 5% CO_2.

Statistical analysis

Analysis and statistical tests were performed using GraphPad Prism, version 6.04 (GraphPad Software, La Jolla, CA, USA).

Results

Anti-FH.07 inhibits AP complement activation

We obtained 21 mouse mAbs, designated anti-FH.01 to anti-FH.21, against plasma-derived human FH. Based on the competition for binding to FH, the mAbs were subdivided in nine groups (**Table 1**). Epitope locations were mapped for eight groups, revealing most mAbs recognized FH at its C-terminal CCP domains. All mAbs binding to N-terminal epitopes of FH also recognized the splice variant FHL-1, while all mAbs directed against CCP18-20 also reacted with FHR-1. All mAbs were tested in standard complement activation assays to investigate their effect on complement regulation, either through determining C3b deposition on activating surfaces or using a hemolytic assay as read-out (**Fig. 1a**, **1b** and **Supplemental Fig. 1**). Most mAbs increased C3b deposition during incubation of 10% (v/v) NHS on either immobilized zymosan or lipopolysaccharide (represented by anti-FH.09 in **Fig. 1a** and **1b**). One mAb, anti-FH.07 (binding to CCP18 of FH, **Supplemental Fig. 2a** and **2b**), decreased

Table 1 Mouse monoclonal antibodies directed against FH used in this study

Designation	Isotype	Epitope location (CCP domain)[a]	Cross-reactivity	Functional effect[b]
Anti-FH.02	Mouse IgG1, Kappa	20	FHR-1	Strong inhibition
Anti-FH.03	Mouse IgG1, Kappa	unknown	FHL-1	Weak inhibition
Anti-FH.07	Mouse IgG1, Kappa	18	FHR-1	Potentiation
Anti-FH.09	Mouse IgG1, Kappa	6	FHL-1, FHR-3, FHR-4A	Strong inhibition
Anti-FH.10	Mouse IgG1, Kappa	20	FHR-1	Strong inhibition
Anti-FH.11	Mouse IgG2a, Kappa	1-4	FHL-1	Strong inhibition[c]
Anti-FH.15	Mouse IgG1, Kappa	5	FHL-1	Strong inhibition
Anti-FH.16	Mouse IgG1, Kappa	16-17	None	Weak inhibition
Anti-FH.19	Mouse IgG1, Kappa	20	FHR-1	Strong inhibition

[a]Epitope location of each mAb was mapped by determining reactivity to FH fragments (**Supplemental Figure 2**). [b]Effect of mAbs on FH function was assessed with standard complement activation assays, see **Figure 1A, 1B** and **Supplemental Figure 1**. [c]Anti-FH.11 inhibits the cofactor activity of FH.

C3b deposition on both surfaces in a dose-dependent manner. This inhibition was also achieved with Fab' fragments of anti-FH.07 (IC_{50} = 0.102 ±0.046 μM), although intact anti-FH.07 was more potent (IC_{50} = 0.046 ±0.011 μM, **Fig. 1c**). This difference in IC_{50} values reflects the presence of two antigen-binding sites in intact IgG compared to one in the Fab' fragment.

FH inhibits fluid phase C3 activation and consumption, which would otherwise decrease functional C3 levels. To investigate the possibility that anti-FH.07 decreased complement deposition through increased C3 consumption in fluid phase, we determined whether anti-FH.07 affected the cofactor activity of FH for FI. In addition, we measured C3b/c levels in NHS following incubation with anti-FH.07. C3b/c is an activation product of C3 and increased levels reflect consumption of C3 due to complement activation or decreased fluid phase regulation[31]. In these experiments anti-FH.07 was compared to anti-FH.11 which binds an epitope in the first four CCP domains, essential for the cofactor activity. Anti-FH.11 blocked

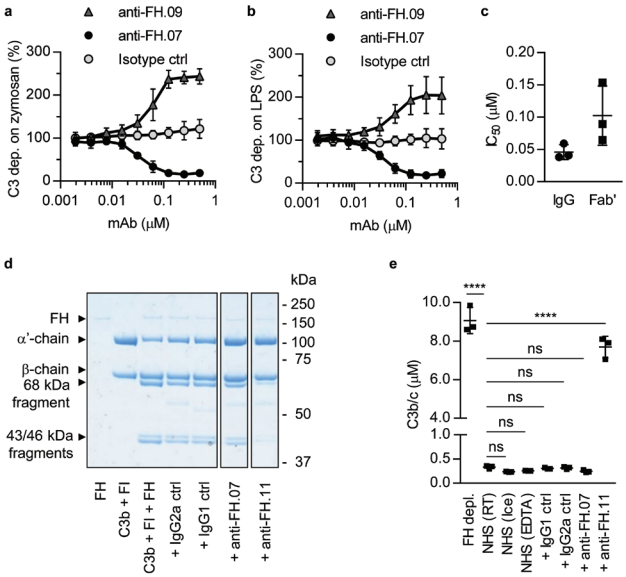

Figure 1 Effect of anti-FH.07 on *in vitro* AP complement activation. AP-mediated C3b deposition on immobilized zymosan (**a**) or LPS (**b**) incubated with 10% (v/v) NHS in the presence of anti-FH.07 (binding CCP18) or anti-FH.09 (binding CCP6), as determined by ELISA. C3b deposition without addition of mAbs was set to 100%. (**c**) IC_{50} of intact or Fab' fragments of anti-FH.07 in the AP-mediated C3b deposition assay on immobilized LPS. (**d**) Fluid phase regulation by FH was assessed with a fluid phase cofactor activity assay. Purified C3b was incubated with FH and FI, with addition of the indicated mAbs (anti-FH.11 binds CCP1-4). Cleavage of the α'-chain of C3b was visualized with SDS-PAGE run under reducing conditions, stained with PageBlue. Lanes were run on the same gel but were noncontiguous. (**e**) C3b/c concentration determined by ELISA after incubation of NHS with the indicated mAbs to assess fluid phase activation of C3. Data in **a**, **b**, **c** and **e** are presented as mean of n=3 with standard deviation. ns: not significant, ****p<0.0001, one-way ANOVA.

C3b α'-chain degradation, whereas anti-FH.07 did not inhibit the cofactor activity of FH for FI, as degradation did not decrease (**Fig. 1d**). As expected, incubating NHS with anti-FH.11 significantly increased C3b/c levels (p<0.0001), comparable to FH depletion (**Fig. 1e**). C3b/c levels remained at background levels after incubation with anti-FH.07. Together, the results show that anti-FH.07 does not inhibit FH and decreases complement activation on surfaces in a FH-dependent manner.

We assessed the binding affinity of anti-FH.07 for FH by SPR. Full length FH was bound by immobilized anti-FH.07 (K_D=5.02*10^{-9} M, **Supplemental Fig. 3a**), but binding fitted poorly to a classical 1:1 model. This might be caused by the presence of various conformations of FH, which bind differently to anti-FH.07. To circumvent this, we also determined the binding of a FH fragment consisting of CCP18-20 (FH_{18-20}) to anti-FH.07. Within this triple domain construct the anti-FH.07 epitope is likely liberated from the complex conformation within the full-length FH molecule. Indeed, using FH_{18-20} resulted in binding curves fitting well to a 1:1 binding model and revealed a higher affinity of anti-FH.07 for domain 18 than found for full length FH (K_D=0.36*10^{-9} M, **Supplemental Fig. 3b**).

FH binding to C3b is enhanced by anti-FH.07

Next, we investigated whether the improved surface regulation of FH induced by anti-FH.07 Fab' fragments involved the binding of FH to C3b, using SPR. The binding affinity, determined by equilibrium analysis, of FH for C3b was similar to those previously reported (K_D=3.21*10^{-6} M), whereas binding to the control ligands iC3b or C3d was very limited (**Fig. 2a** and **Supplemental Fig. 4a**).[36] However, while having corrected for the increased molecular weight of the FH:anti-FH.07 Fab' complex (205 kDa vs 155 kDa for FH alone), the binding of FH to C3b, iC3b and C3d was greatly increased in the presence of Fab' fragments of anti-FH.07 (C3b K_D=1.25*10^{-6} M) (**Fig. 2b** and **Supplemental Fig. 4b**). Although anti-FH.07 enhances FH binding to all three ligands, the increased C3b binding is likely involved in the

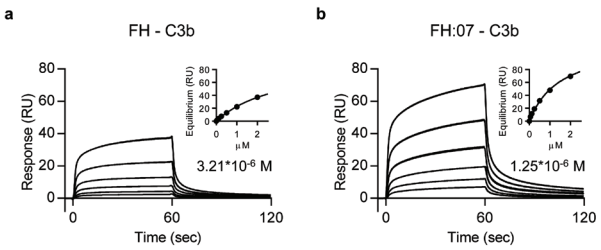

Figure 2 Effect of anti-FH.07 Fab' fragment on binding of FH to C3b. Binding of FH in the absence (**a**) or presence of 4 μM anti-FH.07 Fab' fragments (**b**) to C3b (2,045 RU) Sensograms are normalized for the MW of FH (155 kDa) or the FH:anti-FH.07 Fab' fragment complex (205 kDa), respectively. Insets depict the concentration to response at equilibrium plots at steady state, obtained by measuring RU in the last 5 seconds of injection, with corresponding KD values. All graphs shown are representative of multiple experiments (n≥2). RU: response units.

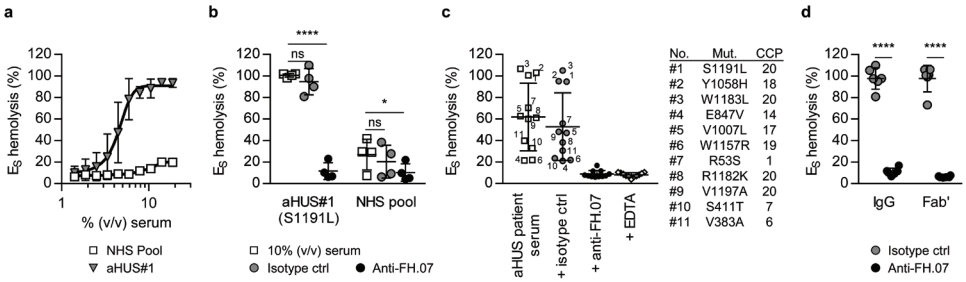

Figure 3 Anti-FH.07 restores complement regulation in aHUS patient serum on sheep erythrocytes. (**a**) Hemolysis of sheep erythrocytes (E_S) by serum from an aHUS patient carrying a heterozygous mutation in *CFH* (n=2) or a serum pool from healthy individuals (NHS pool, n=3). The hemolysis observed by incubation of E_S with 0.6% (w/v) saponin was set to 100%. (**b**) Addition of anti-FH.07 or an isotype control to 10% (v/v) serum of aHUS #1 or a NHS pool (n=4). (**c**) Hemolysis by sera (10%, v/v) of eleven aHUS patients with different *CFH* mutations before and after addition of anti-FH.07 or an isotype control. Numbers correspond to the aHUS patient number listed on the right with corresponding mutations. Addition of EDTA serves as the negative control of E_S lysis. Each point represents the mean of duplicates of a single experiment. (**d**) Comparison of the effect intact IgG and Fab' fragments from a control IgG mAb and anti-FH.07 in the E_S hemolytic assay performed with 10% (v/v) aHUS#1 serum. Data are presented as mean with standard deviation. ns: not significant, *p<0.05, **p<0.01, ****p<0.0001, two-way ANOVA.

underlying mechanism that improves FH activity.

Complement regulation in aHUS patient sera is restored by anti-FH.07

Human FH protects sheep erythrocytes (E_S) from human complement-mediated lysis, providing a well-known model to study FH function on a cell surface[27]. We obtained pre-treatment serum from eleven aHUS patients with unique heterozygous mutations in FH to test the effect of anti-FH.07 on complement-mediated lysis of E_S caused by impaired FH-mediated complement regulation. As expected, E_S were lysed in a dose-dependent manner when incubated with aHUS#1 serum, carrying a heterozygous FH mutation in domain 20 (S1191L) (**Fig. 3a**). In contrast, incubation with a NHS pool containing fully functional FH resulted in 20% lysis. Addition of anti-FH.07 to aHUS#1 serum significantly decreased complement-mediated E_S hemolysis (p<0.0001, **Fig. 3b**). In fact, anti-FH.07 was also effective in NHS, reducing the relatively low background E_S hemolysis from 27% to 10% (p<0.05). Anti-FH.07 decreased lysis to background levels in all aHUS sera, despite variation in initial E_S hemolysis (**Fig. 3c**). As expected[27], mutations located in CCP18-20 of FH caused medium to high E_S hemolysis, but hemolysis was likely also influenced by individual variation in total complement activity of each aHUS serum. In line with the previous experiments, anti-FH.07 Fab' fragments prevented E_S hemolysis in aHUS#1 serum (**Fig. 3d**).

Anti-FH.07-mediated protection is independent of FHR-1 and surface specific

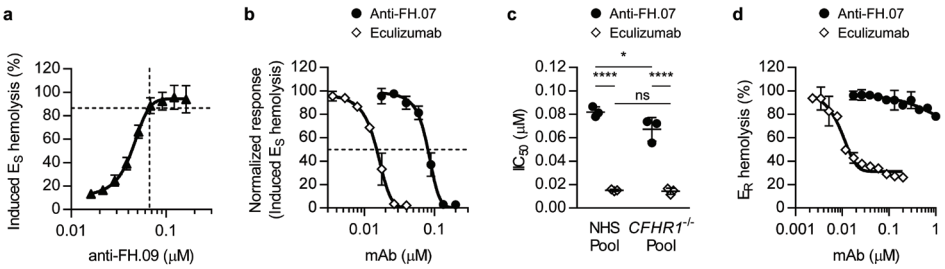

Figure 4 Anti-FH.07 protects sheep erythrocytes from induced complement-mediated hemolysis. (**a**) E_S hemolysis was induced in 10% (v/v) NHS by inhibiting FH with anti-FH.09 (n=3). The hemolysis observed by incubation of E_S with 0.6% (w/v) saponin was set to 100%. (**b**) Titration of anti-FH.07 and eculizumab in the induced E_S hemolysis assay (n=3), after normalization. For this E_S hemolytic assay, 0.067 μM (10 μg/mL) anti-FH.09 was used, resulting in 87% E_S lysis as indicated with the dashed lines in **a**. Dashed line indicates 50% of the normalized E_S hemolysis. (**c**) IC_{50} values of anti-FH.07 and eculizumab in the induced E_S hemolytic assay as in **b** (n=3), using either a NHS pool, or a pool of sera from four healthy donors lacking the *CFHR1* gene (*CFHR1*-/- pool). (**d**) Incubation of rabbit erythrocytes (E_R) with 10% (v/v) NHS serum in the presence of eculizumab or anti-FH.07 at the indicated concentrations (n=2). All data are presented as mean with standard deviation. ns: not significant, **p*<0.05, ***p*<0.01, *****p*<0.0001, two-way ANOVA.

To further investigate the effect of anti-FH.07 on E_S hemolysis, and because aHUS sera are limiting both in availability and complement activity, we developed an induced E_S hemolytic assay using NHS in which FH was inhibited with anti-FH.09. Addition of 0.067 μM (10 μg/mL) anti-FH.09 to 10% (v/v) NHS resulted in 87% E_S hemolysis, similar to the aHUS sera (**Fig. 4a**). Anti-FH.07 completely prevented the induced E_S hemolysis (**Fig. 4b**). This assay allows investigating the complement-inhibiting activity of anti-FH.07 under more controlled conditions and comparing it with eculizumab. Eculizumab inhibited E_S lysis more efficiently (IC_{50}=0.015 μM) compared to anti-FH.07 (IC_{50}=0.082 μM) (**Fig. 4b** and **4c**).

The targeted domain of anti-FH.07, CCP18, is highly similar to CCP3 of FH-homologue FH-related 1 (FHR-1). As anti-FH.07 cross-reacts with FHR-1 (**Supplemental Fig. 2c**), it is possible that the protective effect of anti-FH.07 is due to its interaction with FHR-1 instead of FH. Therefore, we investigated whether in the absence of FHR-1, anti-FH.07 still protects E_S against complement-mediated lysis. E_S hemolysis was induced in a serum pool from four healthy donors previously typed as FHR-1 deficient due to the homozygous *CFHR3/CFHR1* deletion (*CFHR1*$^{-/-}$ pool)[29]. Without FHR-1, anti-FH.07 still prevented E_S hemolysis (**Fig. 4c**, **Supplemental Fig. 5a** and **5b**). Eculizumab was equally effective in the NHS pool and the *CFHR1*$^{-/-}$ pool, whereas anti-FH.07 was more effective in the *CFHR1*$^{-/-}$ pool (IC_{50}=0.067 μM, p<0.05), suggesting that a small portion of anti-FH.07 added to the NHS pool was saturated with FHR-1. More importantly, these results show that FHR-1 is not involved in the protective effect of anti-FH.07.

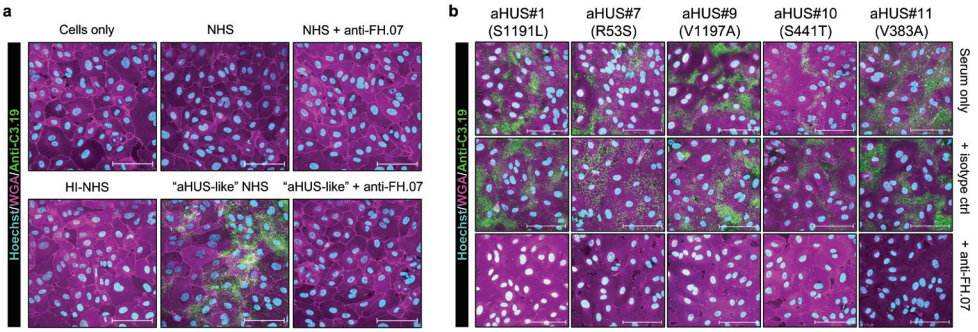

Figure 5 Anti-FH.07 increases complement regulation on human cell surfaces. (**a**) Immunofluorescent imaging of C3b deposition on human umbilical vein endothelial cells (HUVECs) incubated with 10% (v/v) NHS, heat-inactivated NHS (HI-NHS), or "aHUS-like" NHS in the absence or presence of anti-FH.07. For each condition, a representative image of independent experiments (n=3) is shown. (**b**) Immunofluorescent imaging of C3b deposition on HUVECs following incubation with 10% (v/v) serum of five aHUS patients, in the absence of presence of an isotype control mAb or anti-FH.07. HUVECs were stained with Hoechst (turquois, nuclei), WGA (magenta, plasma membrane) and anti-C3.19 (green, C3b deposition). Scale bars represents 100 µm.

In contrast to E_S, rabbit erythrocytes (E_R) do not bind human FH and are lysed when incubated with NHS. E_R were used to investigate whether anti-FH.07 confers FH-mediated regulation to cells that normally are not effectively protected against human complement. E_R remained fully susceptible to AP-mediated hemolysis even in the presence of high amounts of anti-FH.07, whereas eculizumab inhibited E_R hemolysis with an IC_{50} of 0.008 µM (**Fig. 4d**). These results indicate that anti-FH.07-potentiated FH still requires polyanionic residues to bind cells.

Complement activation on human cells is inhibited by anti-FH.07

Next, we determined whether impaired complement regulation on human cells was also restored by anti-FH.07. The "aHUS-like" NHS pool, in which FH was partially inhibited with anti-FH.09, was used to induce complement activation on HUVECs. Incubation of HUVECs with NHS did not result in any significant C3b deposition, although overall relative C3 deposition levels seemed somewhat higher compared to HI-NHS (**Fig. 5a** and **Supplemental Fig. 6**). C3b deposition was greatly increased with "aHUS-like" NHS. This could be completely prevented by anti-FH.07 ($p<0.05$), restoring C3b deposition to background levels. Having established a HUVEC-based FH functional assay, C3b deposition using five aHUS sera was determined. Incubation of HUVECs with aHUS sera resulted in clear C3b deposition, reflecting the impaired FH function (**Fig. 5b**). Anti-FH.07 prevented C3b deposition in all aHUS sera, independent of the FH mutation.

Anti-FH.07 allows normal complement-mediated bacterial killing

To examine whether anti-FH.07 affected complement-mediated killing of bacteria, the

bactericidal activity of NHS against *Escherichia coli* and *N. meningitidis* in the presence of anti-FH.07 or eculizumab was tested. *E. coli* were killed in NHS, while HI-NHS did not show any bactericidal activity (**Fig. 6a**). As expected, eculizumab prevented, in a dose-dependent manner, the killing of *E. coli* in NHS. In contrast, complement-mediated killing of *E. coli* remained fully intact when anti-FH.07 was added (p<0.0001). Similar results were obtained with both *N. meningitidis* serogroup B and W (**Fig. 6b**). Again, eculizumab promoted survival, whereas anti-FH.07 did neither affect killing of *N. meningitidis* serogroup B (p<0.0001) nor W (p<0.01). Of note, eculizumab prevented complement-mediated killing of bacteria at 0.2 μM

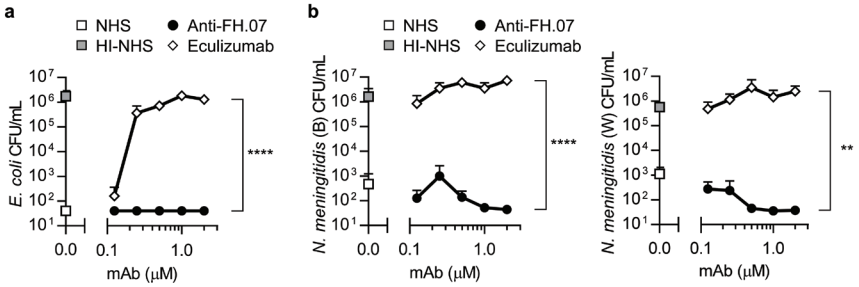

Figure 6 Bactericidal activity of NHS remains intact in the presence of anti-FH.07. (**a**) *Escherichia coli* colony forming units (CFU/mL) were determined after incubation in 75% (v/v) NHS, NHS pre-incubated with anti-FH.07, NHS pre-incubated with eculizumab, or heat-inactivated NHS (HI-NHS). (**b**) CFU/mL of two clinical isolates of *Neisseria meningitidis* serogroup B (left panel) and serogroup W (right panel), determined after incubation in 75% (v/v) NHS, NHS pre-incubated with anti-FH.07, NHS pre-incubated with eculizumab, or HI-NHS. All data are presented as mean with standard deviation (n=3) **p<0.01, ****p<0.0001, two-way ANOVA.

in 75% (v/v) NHS, which is the same ratio as seen in the E_S hemolytic assay in which 0.027 μM in 10% (v/v) NHS was effective. In contrast, anti-FH.07 did not prevent complement-mediated killing of bacteria at 2.0 μM in 75% (v/v) NHS, which is a two-fold higher ratio than the 0.133 μM in 10% (v/v) NHS that was effective in the hemolytic assay.

Discussion

Excessive complement activation on human (endothelial) cells can lead to severe disease - such as aHUS - and there is an increasing interest in complement targeting therapeutics to resolve this. However, inhibiting the detrimental effects of unwanted complement activation while preserving the beneficial protective role against pathogens is an ongoing challenge. Here we investigated the possibility of enhancing the endogenous complement regulator FH and describe a novel approach for inhibiting the complement system. We characterized a mAb, designated anti-FH.07, that binds CCP18 of FH and decreases complement activation in a FH-dependent manner. Anti-FH.07 preserved the specificity of FH, as potentiation

was only observed on cells already able to bind human FH (i.e. sheep erythrocytes and human endothelial cells) and did not confer FH regulation to foreign surfaces such as rabbit erythrocytes and bacteria. Thus, we have discovered a potential novel therapeutic approach for inhibiting complement while preserving the beneficial protective role of complement against pathogens.

It is unclear how anti-FH.07 increases FH function. We ruled out the FH-related proteins or antibody-mediated dimerization as the underlying mechanism of action for anti-FH.07. A truncated form of the major FH-binding protein expressed by *Streptococcus pneumoniae*, PspCN, also enhanced FH activity and induced a conformational change in FH[37]. Anti-FH.07 might also induce such an intra-molecular conformational change or locks FH in a more active conformation. The presence of a latent, closed-up, conformation of FH in the circulation has been previously suggested[22]. In support of this, FH constructs that lack the domains suggested to be involved in the closed-up FH conformation (e.g. CCP10-15 or CCP6-17), were shown to be more effective in surface complement regulation than full-length FH[35,38]. While we don't provide any direct evidence that anti-FH.07 induces such a conformational change in FH, a closed-up conformation of full-length FH would explain the lower binding affinity of full length FH to anti-FH.07, compared with FH_{18-20}. It seems likely that CCP18 of the FH_{18-20} fragment is more accessible in comparison to the closed-up full-length FH molecule. Furthermore, the presence of a latent FH that becomes more active also explains the increased binding of FH to C3b in the presence of anti-FH.07. Anti-FH.07 did not affect the affinity of FH to C3b, but did increase the overall binding, suggesting that not all FH present binds to C3b in the absence of anti-FH.07.

Anti-FH.07 restored the impaired FH function, caused by heterozygous mutations, in aHUS sera. We only tested sera from aHUS patients with heterozygous mutations in *CFH*. Testing anti-FH.07 in aHUS patient sera carrying mutations in *C3* or *CFB*, or with auto-antibodies against FH would provide additional insights in the applicability of FH potentiation. We were not able to test anti-FH.07 in other diseases next to aHUS in this study, but hypothesize potentiating FH would be beneficial in various other complement-mediated diseases and such studies are currently ongoing.

We compared anti-FH.07 with eculizumab in several experimental settings. Eculizumab is a non-depleting therapeutic mAb directed against complement protein C5 and was approved for the treatment of aHUS in 2011[39]. It effectively blocks the initiation of the terminal pathway and thereby inhibits formation of the lytic membrane attack complex (MAC). By inhibiting MAC formation, eculizumab not only protects human cells, but also inhibits complement-mediated lysis of pathogens. Our *in vitro* hemolytic assays showed that preventing complement-mediated lysis requires five-fold less eculizumab compared to anti-

FH.07, suggesting that enhancing FH activity is less effective than inhibiting C5. However, the molar concentrations of the respective targets of eculizumab (C5: 0.4 μM) and anti-FH.07 (FH: 2.0 μM) differ five-fold in serum. When correcting for the concentration difference of the target molecule it seems apparent that despite a different mechanism of action (blocking versus potentiation of the target molecule), similar efficiency in complement inhibition is achieved. Of note, while this suggests that more anti-FH.07, compared to eculizumab, would be required for therapeutic efficacy, it is unknown if all FH molecules need to be potentiated to reach a therapeutic beneficial effect. More importantly, eculizumab also protected bacteria from complement-mediated killing. In contrast, anti-FH.07 did not impair complement-mediated killing of *E. coli* and *N. meningitidis*. This suggests that enhancing FH activity is a more selective, and thus potentially safer, strategy for inhibiting complement in diseases such as aHUS.

In summary, we demonstrate a novel approach for inhibiting complement activation on human cells while preserving the complement-mediated killing of bacteria. This was achieved by enhancing FH activity through targeting CCP18 with mAb anti-FH.07. Both erythrocytes and endothelial cells were protected from complement-mediated damage by anti-FH.07, and it restored the impaired FH function in aHUS patients with different FH mutations *in vitro*. Our results demonstrate FH can be enhanced by targeting CCP18 with a mAb, supporting the hypothesis that FH circulates in a less active form, which can switch into a more active conformation. Demonstrating that FH function can be enhanced while maintaining selectivity for human cells paves the way for developing new therapeutic strategies for inhibiting complement in aHUS.

Author contributions

RBP, MCB, MdG and AEvB performed experiments and analyzed data. RBP, AEvB, TWK and DW designed experiments and interpreted data. PS-C, LvdH, AvdE and CQS provided critical reagents, samples and/or materials and helped to interpret data. RBP, TWK and DW wrote the manuscript. All contributing authors provided critical review of the manuscript and agreed to the submission of this manuscript for publication.

Conflict of interest disclosure

RBP, MCB, TWK and DW are co-inventors of a patent (PCT/NL2015/050584) describing the potentiation of FH with monoclonal antibodies and therapeutic uses thereof, which is licensed to Gemini Therapeutics.

Acknowledgments

We would like to thank all donors and patients that provided material used in this study. We would like to acknowledge Dr. T. Rispens for suggestions and critically reading of the manuscript, and to thank the central facility of Sanquin Research for technical assistance. RBP, AEvB and TWK receive funding from the European Union's seventh Framework program under EC-GA no. 279185 (EUCLIDS; www.euclidsproject.eu). PS-C receives funding from the Spanish "Ministerio de Economía y Competitividad" (PI1200597). Gemini Therapeutics provided partial financial support for this study to RBP and DW.

References

1. Warwicker, P. *et al.* Genetic studies into inherited and sporadic hemolytic uremic syndrome. *Kidney Int.* **53,** 836–844 (1998).
2. Caprioli, J. *et al.* The molecular basis of familial hemolytic uremic syndrome: mutation analysis of factor H gene reveals a hot spot in short consensus repeat 20. *J. Am. Soc. Nephrol.* **12,** 297–307 (2001).
3. Sánchez-Corral, P. *et al.* Structural and functional characterization of factor H mutations associated with atypical hemolytic uremic syndrome. *Am. J. Hum. Genet.* **71,** 1285–1295 (2002).
4. Caprioli, J. *et al.* Complement factor H mutations and gene polymorphisms in haemolytic uraemic syndrome: the C-257T, the A2089G and the G2881T polymorphisms are strongly associated with the disease. *Hum. Mol. Genet.* **12,** 3385–3395 (2003).
5. Dragon-Durey, M.-A. *et al.* Anti-factor H autoantibodies associated with atypical hemolytic uremic syndrome. *J. Am. Soc. Nephrol.* **16,** 555–563 (2005).
6. Rodríguez de Córdoba, S., Tortajada, A., Harris, C. L. & Morgan, B. P. Complement dysregulation and disease: from genes and proteins to diagnostics and drugs. *Immunobiology* **217,** 1034–1046 (2012).
7. Bresin, E. *et al.* Combined complement gene mutations in atypical hemolytic uremic syndrome influence clinical phenotype. *J. Am. Soc. Nephrol.* **24,** 475–486 (2013).
8. Kühn, S. & Zipfel, P. F. Mapping of the domains required for decay acceleration activity of the human factor H-like protein 1 and factor H. *Eur. J. Immunol.* **26,** 2383–2387 (1996).
9. Sharma, A. K. & Pangburn, M. K. Identification of three physically and functionally distinct binding sites for C3b in human complement factor H by deletion mutagenesis. *Proc. Natl. Acad. Sci. U. S. A.* **93,** 10996–11001 (1996).
10. Jokiranta, T. S., Hellwage, J., Koistinen, V., Zipfel, P. F. & Meri, S. Each of the three binding sites on complement factor H interacts with a distinct site on C3b. *J. Biol. Chem.* **275,** 27657–27662 (2000).
11. Blackmore, T. K., Sadlon, T. A., Ward, H. M., Lublin, D. M. & Gordon, D. L. Identification of a heparin binding domain in the seventh short consensus repeat of complement factor H. *J. Immunol.* **157,** 5422–5427 (1996).
12. Blackmore, T. K. *et al.* Identification of the second heparin-binding domain in human complement factor H. *J. Immunol.* **160,** 3342–3348 (1998).
13. Jokiranta, T. S. *et al.* Binding of complement factor H to endothelial cells is mediated by the carboxy-terminal glycosaminoglycan binding site. *Am. J. Pathol.* **167,** 1173–1181 (2005).
14. Józsi, M., Oppermann, M., Lambris, J. D. & Zipfel, P. F. The C-terminus of complement factor H is essential for host cell protection. *Mol. Immunol.* **44,** 2697–2706 (2007).
15. Schmidt, C. Q. *et al.* A new map of glycosaminoglycan and C3b binding sites on factor H. *J. Immunol.* **181,** 2610–2619 (2008).
16. Strobel, S. *et al.* Factor H-related protein 1 neutralizes anti-factor H autoantibodies in autoimmune hemolytic uremic syndrome. *Kidney Int.* **80,** 397–404 (2011).
17. DiScipio, R. G. Ultrastructures and interactions of complement factors H and I. *J. Immunol.* **149,** 2592–2599 (1992).
18. Aslam, M. & Perkins, S. J. Folded-back solution structure of monomeric factor H of human complement by synchrotron X-ray and neutron scattering, analytical ultracentrifugation and constrained molecular modelling. *J. Mol. Biol.* **309,** 1117–1138 (2001).
19. Okemefuna, A. I., Nan, R., Gor, J. & Perkins, S. J. Electrostatic interactions contribute to the folded-back conformation of wild type human factor H. *J. Mol. Biol.* **391,** 98–118 (2009).
20. Okemefuna, A. I. *et al.* The regulatory SCR-1/5 and cell surface-binding SCR-16/20 fragments of factor H reveal partially folded-back solution structures and different self-associative properties. *J. Mol. Biol.* **375,** 80–101 (2008).
21. Makou, E. *et al.* Solution structure of CCP modules 10-12 illuminates functional architecture of the complement regulator, factor H. *J. Mol. Biol.* **424,** 295–312 (2012).
22. Makou, E., Herbert, A. P. & Barlow, P. N. Functional anatomy of complement factor H. *Biochemistry* **52,** 3949–3962 (2013).
23. Merinero, H. M. *et al.* Complete functional characterization of disease-associated genetic variants in the complement factor H gene. *Kidney Int.* 1–12 (2017). doi:10.1016/j.kint.2017.07.015
24. Goicoechea de Jorge, E. *et al.* Factor H competitor generated by gene conversion events associates with atypical hemolytic uremic syndrome. *J. Am. Soc. Nephrol.* **29,** (2018).
25. Tortajada, A. *et al.* Complement factor H variants I890 and L1007 while commonly associated with atypical

hemolytic uremic syndrome are polymorphisms with no functional significance. *Kidney Int.* **81,** 56–63 (2012).
26. Józsi, M. *et al.* Factor H and atypical hemolytic uremic syndrome: mutations in the C-terminus cause structural changes and defective recognition functions. *J. Am. Soc. Nephrol.* **17,** 170–177 (2006).
27. Sánchez-Corral, P., González-Rubio, C., Rodríguez de Córdoba, S. & López-Trascasa, M. Functional analysis in serum from atypical hemolytic uremic syndrome patients reveals impaired protection of host cells associated with mutations in factor H. *Mol. Immunol.* **41,** 81–84 (2004).
28. Davin, J. C. *et al.* Complement factor H-associated atypical hemolytic uremic syndrome in monozygotic twins: concordant presentation, discordant response to treatment. *Am. J. Kidney Dis.* **47,** 27–30 (2006).
29. Pouw, R. B. *et al.* Complement factor H-related protein 3 serum levels are low compared to factor H and mainly determined by gene copy number variation in CFHR3. *PLoS ONE* **11,** e0152164 (2016).
30. Pechtl, I. C., Kavanagh, D., McIntosh, N., Harris, C. L. & Barlow, P. N. Disease-associated N-terminal complement factor H mutations perturb cofactor and decay-accelerating activities. *J. Biol. Chem.* **286,** 11082–11090 (2011).
31. Wolbink, G. J. *et al.* Application of a monoclonal antibody against a neoepitope on activated C4 in an ELISA for the quantification of complement activation via the classical pathway. *J. Immunol. Methods* **163,** 67–76 (1993).
32. Hack, C. E. *et al.* Disruption of the internal thioesther bond in the third component of complement (C3) results in the exposure of neodeterminants also present on activation products of C3: an analysis with monoclonal antibodies. *J. Immunol.* **141,** 1602–1609 (1988).
33. Meulenbroek, E. M. *et al.* Complement deposition in autoimmune hemolytic anemia is a footprint for difficult-to-detect IgM autoantibodies. *Haematologica* **100,** 1407–1414 (2015).
34. Kuijpers, T. W. *et al.* Complement factor 7 gene mutations in relation to meningococcal infection and clinical recurrence of meningococcal disease. *Mol. Immunol.* **47,** 671–677 (2010).
35. Schmidt, C. Q. *et al.* Selectivity of C3-opsonin targeted complement inhibitors: A distinct advantage in the protection of erythrocytes from paroxysmal nocturnal hemoglobinuria patients. *Immunobiology* **221,** 503–511 (2016).
36. Schmidt, C. Q. *et al.* Rational engineering of a minimized immune inhibitor with unique triple-targeting properties. *J. Immunol.* **190,** 5712–5721 (2013).
37. Herbert, A. P. *et al.* Complement evasion mediated by enhancement of captured factor H: implications for protection of self-surfaces from complement. *J. Immunol.* **195,** 000–000 (2015).
38. Harder, M. J. *et al.* Comparative analysis of novel complement-targeted inhibitors, miniFH, and the natural regulators factor H and factor H-like protein 1 reveal functional determinants of complement regulation. *J. Immunol.* **196,** 866–876 (2015).
39. Zuber, J. *et al.* Use of eculizumab for atypical haemolytic uraemic syndrome and C3 glomerulopathies. *Nat. Rev. Nephrol.* **8,** 643–657 (2012).

Supplemental Material

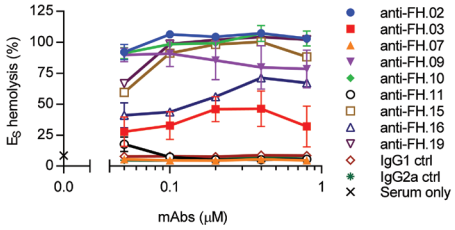

Supplemental Figure 1 Effect of anti-FH mAbs in the sheep erythrocyte hemolytic assay. Sheep erythrocytes (E_S) were incubated in 10% (v/v) normal human serum with the indicated mAbs for 75 minutes. Hemolysis was measured as absorbance at 412 nm, corrected for background absorbance measured at 690 nm and expressed as percentage of the 100% lysis control (E_S incubated with H_2O with 0.6% (w/v) saponin).

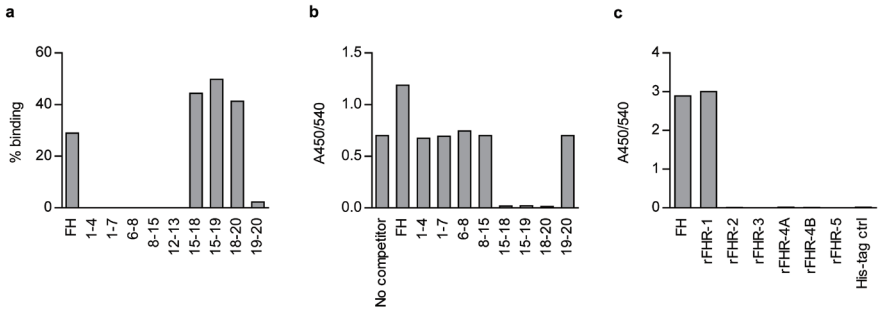

Supplemental Figure 2 Epitope mapping and cross-reactivity of anti-FH.07. (**a**) Binding of ^{125}I-labelled FH and fragments of FH to anti-FH.07 was assessed by radio immuno assay (RIA). Percentage binding was calculated based on the input. (**b**) ELISA-based competition assay using biotinylated FH and unbiotinylated FH or FH fragments. Binding of FH-bt in the presence of 100-fold excess of indicated competitors was determined by ELISA. (**c**) Binding of biotinylated FH or recombinant FHR proteins to anti-FH.07 was determined by ELISA.

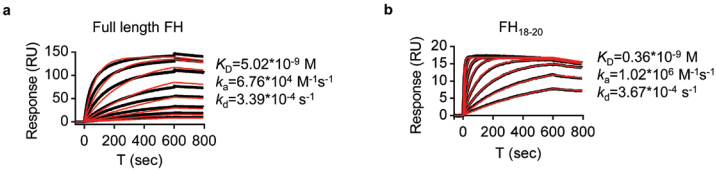

Supplemental Figure 3 Representative SPR sensograms (n=2) of the binding of full length FH (**a**) or a fragment of FH comprised of domains 18 to 20 (**b**) to immobilised anti-FH.07. For full length FH, a two-fold diluting concentration range starting at 200 nM was probed. For FH_{18-20} a two-fold diluting concentration range starting at 150 nM was probed. Injections were done in random order. The first 200 seconds of the 600 seconds dissociation phase are shown. Red lines depict the fits of a 1:1 association model. RU: response units.

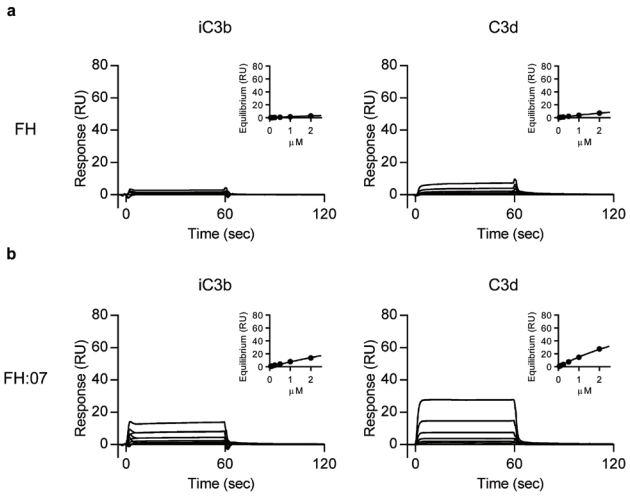

Supplemental Figure 4 Effect of anti-FH.07 Fab' fragment on binding of FH to C3 fragments. Binding of FH in the absence (**a**) or presence of 4 μM anti-FH.07 Fab' fragments (**b**) to iC3b (2,039 RU) and C3d (2,055 RU). Double injections of a two-fold diluting concentration range starting at 2 μM FH were probed, in random order throughout. Sensograms were normalized for the MW of FH (155 kDa) or the FH:anti-FH.07 Fab' fragment complex (205 kDa), respectively. Insets depict the concentration to response at equilibrium plots at steady state, obtained by measuring RU in the last 5 seconds of injection. All graphs shown are representative of multiple experiments (n≥2). RU: response units.

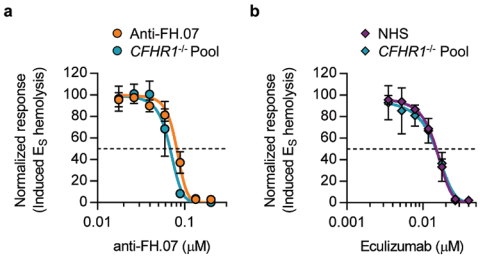

Supplemental Figure 5 Inhibition of complement-mediated hemolysis of sheep erythrocytes by anti-FH.07 in *CFHR1*-/- serum. Sheep erythrocyte (E_S) hemolysis was induced using aHUS-like serum, using either a sera pool from NHS or consisting of sera from donors with a homozygous deletion of CFHR1 (*CFHR1*-/- Pool). Anti-FH.07 was added at indicated concentrations (**a**) or corrected for the respective concentration of FH (**b**). Horizontal dashed lines indicate 50% of the inhibition, vertical dashed lines indicate the corresponding IC_{50} values included in Figure 4 of the main manuscript. All data (n=3) are presented as mean with standard deviation.

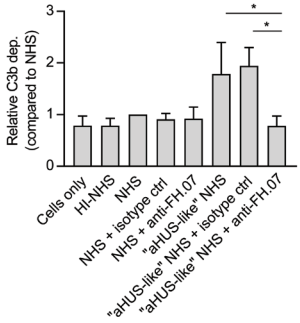

Supplemental Figure 6 Relative C3b deposition on HUVECs, from Figure 5A. Calculated by quantifying the mean fluorescence intensity (MFI) using a maximum intensity projection of the whole coverslip (10x10x15 images per coverslip). Anti-C3.19 MFI of NHS was set to 1. Bars represent mean with standard deviation (n=3). *P<0.05, one-way ANOVE.